Cross sections for He, Li, and Be isotopes produced in the $\alpha+\alpha$ reaction at 198.4 MeV

L. W. Woo, K. Kwiatkowski, S. H. Zhou,* and V. E. Viola
Department of Chemistry and IUCF, Indiana University, Bloomington, Indiana 47405
(Received 1 April 1985)

Cross sections for production of Li and Be isotopes in the $\alpha(\alpha,pn)^6Li$, $\alpha(\alpha,p)^7Li$, and $\alpha(\alpha,n)^7Be$ reactions have been measured at 198.4 MeV. These measurements are relevant to the understanding of light-element nucleosynthesis in galactic cosmic ray interactions with the interstellar medium. The data indicate that beyond energies of about 250 MeV, the $\alpha+\alpha$ reaction does not contribute to the natural abundance of lithium, reinforcing theories which produce ^6Li in cosmic ray processes and most of nature's ^7Li in the big bang. In addition, $\alpha+\alpha$ elastic scattering data obtained in these experiments have been analyzed in terms of the optical model, and the results are compared with lower-energy systematics.

I. INTRODUCTION

While most of nature's elements from carbon through uranium are synthesized during various stages of stellar evolution, the isotopes of the lightest elements—H, He, Li, Be, and B—find their origin in less-dense, more energetic astrophysical environments.[1] Cosmological nucleosynthesis in the big bang[2] is believed to be the major source of ^2H, ^3He, ^4He, and perhaps ^7Li, whereas interactions of galactic cosmic rays (GCR's) with the interstellar medium (ISM) are proposed[3] to account for ^6Li, ^9Be, ^{10}B, and ^{11}B.

The ability of these two models to reproduce the observed abundances of the light elements with a minimum of parameters represents a major success for nuclear astrophysics, and further, infers important consequences concerning the baryon density of the universe.[1] Specifically, the present results are consistent with a baryon density that is too low to close the universe. Hence, assuming negligible mass for the neutrino, studies of light-element nucleosynthesis lead to the conclusion that the universe is open and will expand forever.

One of the major remaining uncertainties in this scenario for light-element creation concerns the isotopic ratio and absolute abundances for lithium. The GCR + ISM model has been shown to be incapable of reproducing the observed isotopic ratio for lithium, $^7Li/^6Li=12.5$, underestimating the ^7Li abundance by an order of magnitude. The required ^7Li, however, can be supplied self-consistently by big bang nucleosynthesis or by other astrophysical processes, provided the GCR + ISM mechanism produces the correct amount of ^6Li. In evaluation of ^6Li production via the GCR + ISM mechanism, cross section data are required for reactions of protons and ^4He ions with ^4He, C, N, and O nuclei over an energy range corresponding to the maximum cosmic ray flux ($\sim 0.1-1$ GeV). With the exception of the $\alpha+\alpha$ reaction, all salient cross sections relevant to this problem are now well characterized.[4]

Lithium production in the $\alpha+\alpha$ reaction has previously been studied up to a bombarding energy of 160 MeV (Refs. 5–7) and also at energies between 400–1000 MeV.[8] These results indicate that $\alpha+\alpha$ collisions provide a major source of nature's ^6Li, but cannot supply the additional ^7Li required to reproduce the observed $^7Li/^6Li$ isotopic ratio. Further, the excitation functions for the $\alpha(\alpha,p)^7Li$, $\alpha(\alpha,n)^7Be$, and $\alpha(\alpha,d)^6Li$ reactions all decrease exponentially at ^4He energies beyond 60 MeV.[7] Hence, these two-body final state reactions cannot yield significant ^6Li and ^7Li at energies above approximately 150 MeV. In addition, the $\alpha(\alpha,2p)^6He$ reaction has been shown to be too small at all energies to be significant.

However, for the three-body final state reaction $\alpha(\alpha,pn)^6Li$, which dominates ^6Li production above 60 MeV, the situation has been uncertain. For ^4He energies between 60 and 140 MeV, the $\alpha(\alpha,pn)^6Li$ cross section is nearly constant, a characteristic feature of multibody final state reactions in light nuclei at energies well above threshold.[4,9] However, studies at 160 MeV suggest the onset of an exponential decrease in this cross section.[7] If this exponential decrease persists to higher energies, then the GCR + ISM mechanism can account for the absolute abundance of ^6Li satisfactorily and the question of light element synthesis can be considered well in hand. If, on the other hand, this cross section should be independent of energy above ~ 140 MeV, then the GCR + ISM model would overproduce ^6Li, leaving the question of light element synthesis clouded.

The objective of the present experiment was to investigate the $\alpha+\alpha$ reaction at the maximum energy available at the Indiana Cyclotron in order to examine the behavior of the ^6He, ^6Li, ^7Li, and ^7Be excitation functions at higher energies. As a by-product of these studies, elastic scattering cross sections were also determined. These latter results are analyzed in terms of an optical model parametrization and then compared with lower-energy studies.[10(a)]

II. EXPERIMENTAL PROCEDURES AND DATA ANALYSIS

These experiments were performed at the Indiana University Cyclotron Facility with a beam of 198.4-MeV

^{4}He ions. Beam intensities varied from 1 nA for forward-angle measurements to 50 nA at the most backward angles. Beam spot size was approximately 2 mm$\times$2 mm, as monitored by a scintillator inserted upstream of the gas target cell. A gas target cell similar in design to that used in Ref. 7 was operated at a pressure of 267 Torr. The cell window thickness was substantially less than the ranges of the lowest energy fragments of interest in these measurements. The interaction volume for the cell and detector solid angle were defined by a multiple slit system. The primary elements were a vertical slit 3.0 mm wide placed 12 cm from the target center for the target definition and detector-defining slits of 6.30 mm$\times$6.25 mm placed at a distance of 51 cm from the target center.

A four-element detector telescope was employed for mass, charge, and energy identification of ^{4}He, ^{6}He, ^{6}Li, ^{7}Li, and ^{7}Be ions. This telescope consisted of three surface-barrier silicon detectors of thicknesses 50 μm, 1 mm, and 2 mm, followed by a 5 mm Si(Li) detector, tilted at 60 deg in order to stop elastically-scattered ^{4}He ions.

Measurements were performed over an angular range from 5 to 34 deg, covering the full kinematic range for $A=6$ and 7 fragments. Due to the limitations of low counting rate and available beam time, it was not possible to cover the 34—45 deg range for elastic ^{4}He ions. The absolute zero angle of the beam axis was determined by left-right asymmetry measurements of elastically-scattered ^{4}He ions. In addition, a monitor telescope consisting of a 1-mm silicon surface barrier ΔE detector and a NaI E detector was used to check the consistency of the beam integrator and target cell pressure values.

Standard linear and logic electronics were employed and a pulse generator was fed into all preamplifiers in order to monitor detector gains and deadtime losses. From ΔE-E particle-identification spectra the mass and charge of each fragment could be unambiguously defined for all products of the $\alpha+\alpha$ reaction. Blank runs were performed with the target cell evacuated in order to evaluate possible sources of Li and Be ions produced in the cell windows or other anomalous scattering sites in the scattering chamber. Corrections for such effects were found to be negligible. Possible contamination of the spectra due to impurities in the ^{4}He gas could be estimated from observation of any non-two-body state ^{7}Li and ^{7}Be fragments, as well as any $A \geq 8$ fragments in the spectra. Gas impurities were a problem only for the ^{6}Li spectra at backward angles, where the differential cross sections were quite low. These data were corrected assuming the impurities were due to carbon or oxygen contamination and using the cross section and energy spectra for ^{4}He-induced reactions on these elements of Gökmen *et al.*[10(b)] to scale any such background from $A=7$ to $A=6$. This background was included in quadrature in the error propagation procedure for these data. The energy resolution in these measurements was not sufficient to separate the excited states of ^{7}Li and ^{7}Be. Because of the kinematics of the two-body final state reactions (α,p), (α,n), and (α,d), each measurement yielded both forward (c.m.) and backward (c.m.) differential cross section data (except when the energy of the backward-emitted fragment was too low to penetrate the 50 μm detector element). The angular distributions for the (α,n) and (α,p) reactions are shown in Fig. 1 and the (α,d) results are shown in Fig. 2. Elastic scattering results appear in Fig. 3.

Differential cross sections for the $\alpha(\alpha,pn)$ reaction, which leads to a continuum of final states involving both forward- and backward-emitted fragments, were derived as in Ref. 7. In this procedure it is assumed that the

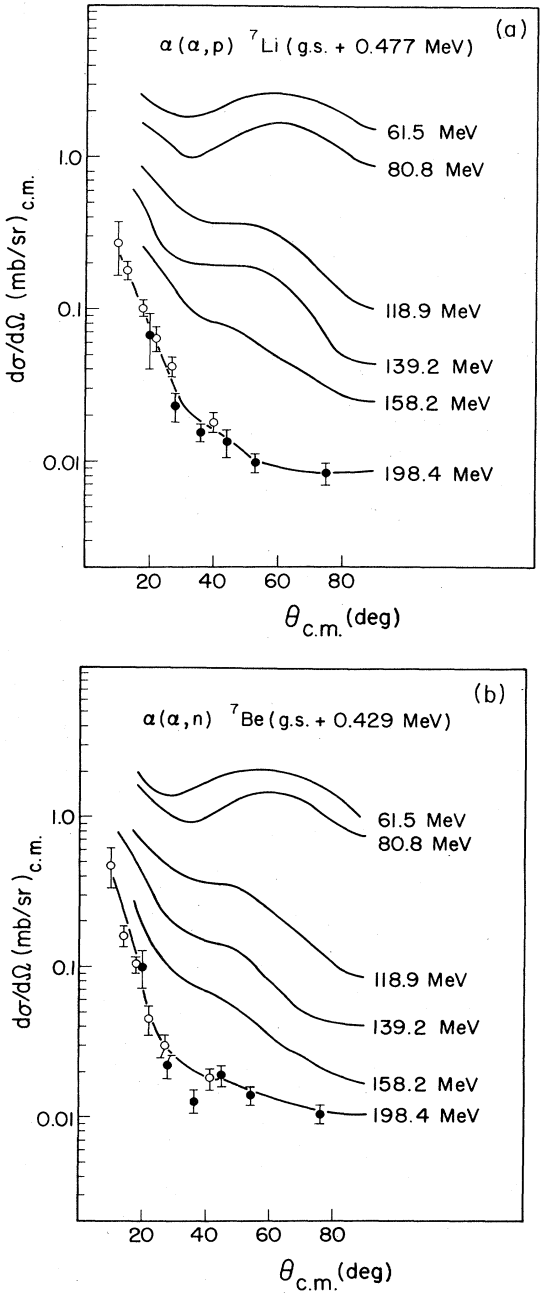

FIG. 1. Center-of-mass angular distribution of ^{7}Li and ^{7}Be (ground state plus first excited state) from the $\alpha+\alpha$ reaction at 198.4 MeV. Solid points refer to forward (c.m.) hemisphere and open points to backward hemisphere data. Solid lines summarize lower-energy data from Ref. 7 except lower line, which is to guide the eye through the present data.

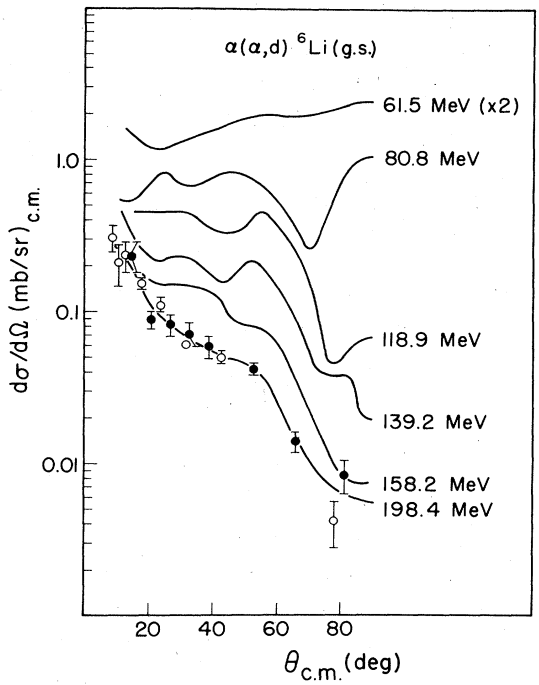

FIG. 2. Center-of-mass angular distribution of $\alpha(\alpha,d)^6Li$ (ground state) from the $\alpha+\alpha$ reaction at 198.4 MeV. Solid points refer to forward (c.m.) hemisphere and open points to backward hemisphere data. Solid lines summarize lower-energy data from Ref. 7, except lower line, which is to guide the eye through the present data.

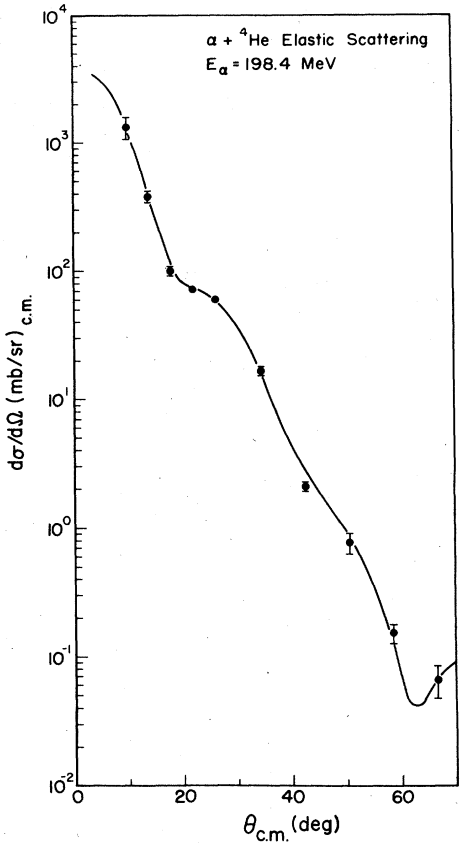

FIG. 3. Elastic scattering angular distribution from the $\alpha+\alpha$ reaction at 198.4 MeV. Solid line is optical-model fit with parameters of Table III, using the WS1 + WS2 potential.

kinematic behavior of ^6Li fragments corresponds to two-body breakup involving "pseudo-excited states" of ^2H. This then defines a locus of ^6Li energies corresponding to 90 deg (c.m.) as a function of laboratory angle. All energies greater than this value in a given spectrum were attributed to the forward hemisphere cross section, while lower energies were assigned to the backward component. In all cases, contributions from the (α,d) peak in the energy spectrum were subtracted from the continuum. We estimate the error due to this procedure to be about 10 percent, which is included in the error propagation for the ^6Li three-body state cross sections. Cross sections for ^6He production were below the detection limits of our system in this experiment. The total cross sections for these reactions are tabulated in Table I.

III. RESULTS FOR $A=6$ AND 7: ASTROPHYSICAL IMPLICATIONS

The center-of-mass differential cross sections for the two-body final state reactions are shown in Figs. 1 and 2, along with curves representing experimental data obtained at lower energies. For ^7Be and ^7Li the angular distributions continue to develop a strong forward peaking. The shoulder present near 45—60 deg in the lower-energy data has disappeared completely at an energy of 198 MeV. Attempts to fit these data with existing theoretical models are made difficult by the inability to distinguish between the ground and first-excited states in these spectra. The $(\alpha,d)^6Li$ data also exhibit continued development of a deep minimum near 90 deg, consistent with the evolution of the lower-energy angular distributions. These data have been previously described moderately well[7] by two-nucleon-transfer DWBA calculations using the finite range code MARY2,[11] which are also consistent with the results obtained in this work.

The measured total cross sections for all processes leading to the formation of $A=6$ and 7 isobars are listed in Table I. These values are combined with lower-energy data, summarized in Ref. 4, to yield the excitation functions for ^6Li, ^7Li, and ^7Be production in the $\alpha+\alpha$ reaction

TABLE I. Total cross sections for $A=6$ and 7 isobars from the $\alpha+\alpha$ reaction at 198.4 MeV.

	$(\alpha,2p)^6He$	$(\alpha,d)^6Li$	$(\alpha,pn)^6Li$	Total ^6Li	$(\alpha,p)^7Li^a$	$(\alpha,n)^7Be^a$
σ (mb)	<0.2	0.6 ± 0.2	2.8 ± 0.7	3.4 ± 0.8	0.25 ± 0.06	0.35 ± 0.08

[a]Ground state plus first excited state.

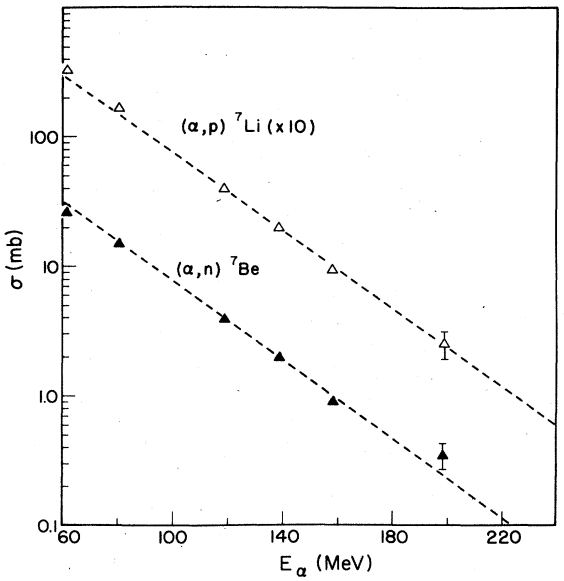

FIG. 4. Excitation functions for $A=7$ production in the $\alpha+\alpha$ reaction. Symbols are as follows: △—^{7}Li, multiplied by ten; ▲—^{7}Be. Dashed line is Eq. (4).

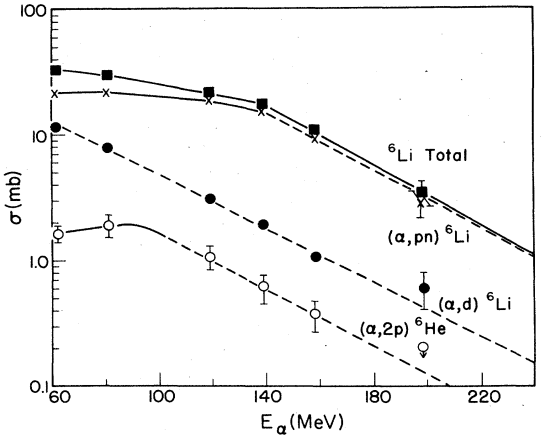

FIG. 5. Excitation functions for $A=6$ production in the $\alpha+\alpha$ reaction. Symbols are as follows: ○—$\alpha(\alpha,2p)$; ●—$\alpha(\alpha,d)$; ×—$\alpha(\alpha,pn)$; ■—total $A=6$. Dashed lines are Eqs. (1)—(3), respectively. Solid lines are to guide the eye.

shown in Figs. 4 and 5. Of particular significance to the objectives of this research, it is observed that the $\alpha(\alpha,pn)^6$Li reaction continues to dominate ^{6}Li production at high energies, but that this cross section decreases with increasing energy, as indicated by the data of Ref. 7. This result suggests that unlike reactions on more complex light nuclei, the three-body final state reaction in $\alpha+\alpha$ collisions follows the same exponential decrease at high energies as do the two-body final states.

Also shown in Figs. 4 and 5 are fits to the high-energy portion of each excitation function (dashed lines) leading to $A=6$ and 7 formation. These are given by the following expressions:

$$\sigma(^6\text{He})=20e^{-0.025E}\ (E>100\ \text{MeV})\ , \tag{1}$$

$$\sigma(^6\text{Li}_\text{d})=59e^{-0.025E}\ (E>60\ \text{MeV})\ , \tag{2}$$

$$\sigma(^6\text{Li}_\text{pn})=500e^{-0.025E}\ (E>140\ \text{MeV})\ , \tag{3}$$

$$\sigma(^7\text{Li},^7\text{Be})=260e^{-0.035E}\ (E>60\ \text{MeV})\ , \tag{4}$$

where σ is in millibarns and E is the bombarding energy for ^{4}He in the laboratory system. One notes that for the two-body final state reactions the exponential dependence sets in at a much lower energy than for the three-body final states.

In terms of Li nucleosynthesis these results reinforce the previous conclusion that beyond ^{4}He energies of about 250 MeV, the $\alpha+\alpha$ reaction does not contribute significantly to ^{6}Li and ^{7}Li synthesis.[7] Further, the excitation functions of Figs. 4 and 5 demonstrate that any nonthermal mechanism which employs conventional H/He/CNO abundances cannot reproduce the ^{7}Li/^{6}Li abundance ratio of 12.6. The exception to this would be a monoenergetic flux spectrum with a very narrow energy window (≤ 1 MeV) near the $\alpha+\alpha$ threshold.[12,13]

In order to examine the influence of these new data on ^{6}Li and ^{7}Li nucleosynthesis via the GCR + ISM mechanism, calculations have recently been performed[13] using a leaky-box model.[14,15] This calculation includes cross sections from a recent review of all data relevant to Li, Be, and B nucleosynthesis,[4] as well as new abundance tables for the interstellar medium.[16,17] In these calculations it is assumed that the galactic lifetime is 10^{10} yr and the cosmic ray mean path for escape is 5 g/cm^2. To examine the limits on ^{6}Li production established by the present data, two assumptions are included concerning the (α,pn) cross section above 200 MeV: (1) the exponential decrease given in Eqs. (2) and (3), and (2) a constant value of 3.4 mb for all energies above 200 MeV. The results of this calculation are given in Table II, where they are compared with experimental abundances for Li, Be, and B isotopes taken

TABLE II. Lithium abundance ratios predicted by galactic cosmic ray plus interstellar medium model (Ref. 13). All abundances are relative to $H=10^{12}$ atoms. Parentheses indicate error factors for experimental values.

	^{6}Li	^{7}Li	^{7}Li/^{6}Li	^{6}Li/^{9}Be	B/^{6}Li
expt[a]	70(2)	900(2)	12.6±0.2	5.0(3)	2.2(3)
calc[b]	110	160	1.4	7.3	2.3
calc[c]	130	160	1.2	8.6	1.9

[a]Reference 1.
[b]Assumes $\sigma(^6\text{Li})$ from Eqs. (2) and (3).
[c]Assumes $\sigma(^6\text{Li})=3.4$ mb for all $E_\alpha>200$ MeV.

from Ref. 1. It should be noted that the abundance tables of Cameron[16] and Anders[17] quote values for Li, Be, and B in excess of a factor of 2 larger than those of Austin.[1] The primary difference between these compilations is that Refs. 16 and 17 place predominant weight on meteoritic Li, Be, and B measurements, whereas Austin gives primary weight to photospheric abundances. While both sets are within experimental errors, we have chosen to emphasize the photospheric values here, following the precedent of several earlier Li, Be, and B abundance evaluations.[18–20]

With respect to the absolute abundance of ^{6}Li, the calculations for both $\alpha+\alpha$ cross section assumptions agree with the data within the limits of error. However, since the constant cross section assumption yields a result which is at the upper bound of the experimental uncertainty, measurement of the $\alpha(\alpha,^6\mathrm{Li})$ cross section at about 250 MeV bombarding energy range would appear to be useful in reducing this uncertainty even further. The model calculations also give quite satisfactory agreement with the observed elemental abundance ratios, ^{6}Li/^{9}Be and B/^{6}Li, well within the error factors for these ratios. It should be noted that the present calculations reproduce the absolute ^{9}Be abundance within 5 percent. Since this isotope is subject to the smallest uncertainties, both in terms of experimental and calculated values, this concordance is reassuring. Hence, the present study reinforces previous conclusions that Li, Be, and B (but not the observed ratio ^{11}B/^{10}B) can be well accounted for by the GCR + ISM mechanism and demonstrates that overproduction of ^{6}Li by the $\alpha+\alpha$ reaction is not a serious problem for the model.

The inability of the GCR + ISM model to account for the well-established ^{7}Li/^{6}Li ratio (Table II) has long been recognized. The results of the present measurement simply amplify this discrepancy. Since ^{7}Li is also produced in big bang nucleosynthesis, the ^{7}Li/^{6}Li isotopic ratio can be most easily understood in terms of a model in which the major source of ^{7}Li is the big bang and that for ^{6}Li is the GCR + ISM mechanism. In fact, using the standard model and a universal baryon density which reproduces the observed ^{2}H, ^{3}He, and ^{4}He abundances, cosmological nucleosynthesis in the big bang and GCR interactions with the ISM can successfully account for all light element nucleosynthesis in a quantitative fashion.

One possible discordant note in this otherwise harmonious scenario has recently been provided by measurements of the Li abundance in extreme population II dwarf stars, in particular halo dwarfs.[21] These objects are very old, very metal-poor stars which are argued to be representative of primordial, pregalactic material. In Ref. 21 a value of $N_{\mathrm{Li}}/N_{\mathrm{H}}=112\pm38\times10^{-12}$ is observed, a value nearly eight times smaller than the value of $N_{\mathrm{Li}}/N_{\mathrm{H}}=900\times10^{-12}$ listed in Table II. If this value is accepted as the contribution of the big bang to the present-day ^{7}Li abundance, then an additional mechanism must supply a major fraction of nature's ^{7}Li, e.g., synthesis during the novae phase of stellar evolution. However, the results of Ref. 21 are subject to errors beyond the quoted statistical values, primarily related to astration (^{7}Li destruction) in the proto-stellar and subsequent environment and assumptions involved in the models of stellar atmospheres. The former error is estimated to be about a factor of 3 and the latter a factor of 2, leading to a factor of 6 total uncertainty.[21] Combining all errors, and allowing for one standard deviation in the statistical error of Ref. 21, the upper bound of the new ^{7}Li measurements remains consistent with the value quoted in Table II. Hence, at this stage there is no compelling reason to abandon the previous scenario for the origin of the light elements. Nonetheless, a note of caution is sounded which warrants careful future examination of these abundances.

Assuming that the measurements of Ref. 21 do not distort our earlier picture, an alternative interpretation of the failure of the GCR + ISM model to reproduce the ^{7}Li/^{6}Li ratio is to demand—*a priori*—that the additional ^{7}Li must come from the big bang. The salient variable in the calculation then becomes the baryon density of the universe. Using this approach, big bang calculations with the standard model[2,22,23] require a baryon density, ρ_B, an order of magnitude lower than the critical density of the universe, ρ_c, in order to produce the required ^{7}Li. Hence, this line of reasoning leads to the conclusion that the universe is open and will expand forever (assuming neutrinos have negligible mass). The results of Ref. 21, taken at face value, only strengthen this conclusion. Even more sensitive estimates of ρ_B, which partially account for effects due to galactic infall and astration, can be obtained by examining the ratio of ^{7}Li to ^{2}H, both of which exhibit a very sensitive dependence on ρ_B.[24]

IV. ELASTIC SCATTERING RESULTS

In addition to measurements of the cross sections for $A=6$ and 7 nuclides produced in this study, $\alpha+\alpha$ elastic-scattering differential cross sections were also obtained, as shown in Fig. 3. Optical model analyses have been applied to these data using two different parametrizations of the real potential. These include:

(i) a strongly attractive Woods-Saxon (WS) potential, as suggested by Neudatchin *et al.*[25] and by Buck *et al.*[26] and

(ii) a sum of two attractive Woods-Saxon terms (WS1 + WS2), successfully used at lower energies.[10]

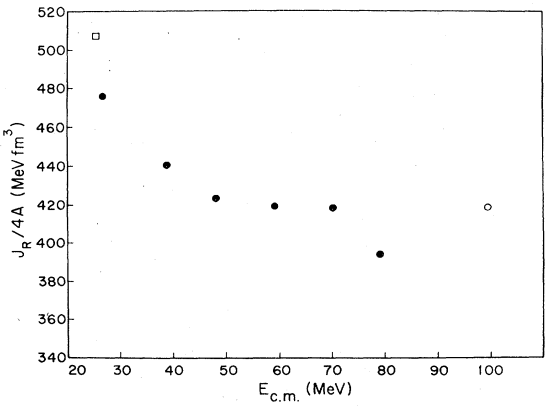

FIG. 6. Real volume integrals from optical model analysis of $\alpha+\alpha$ elastic scattering data. Symbols are as follows: ○—this work; ●—Ref. 10; □—Ref. 27.

TABLE III. Optical-Model parameters used to fit the data in Fig. 3 compared with values for 158.2 MeV, as quoted in Ref. 10. Potentials V and W are in MeV and half-radii r and diffuseness parameters a are in fm.

E_α	V_1	r_1	a_1	W	r_I	a_I	V_2	r_2	a_2	$J_R/4_A$	$J_I/4_A$	X^2/N
198.4[a]	78.6	1.211	0.749	11.6	1.832	0.927				368	150	6.5
198.4[b]	59.2	1.505	0.694	30.1	1.654	0.472	55.8	0.808	0.407	418	188	1.8
158.2[b]	53.8	1.628	0.613	9.6	2.094	0.467	44.0	0.545	0.142	394	112	1.5

[a]Strongly attractive WS potential.
[b]Sum of two attractive WS terms.

In both cases the imaginary potential assumed a standard Woods-Saxon volume absorption shape.

The best fit to the data was obtained with parametrization (ii); i.e., WS1 + WS2, with a chi-squared-per point value χ^2/N of 1.8. The standard optical model form (i) exhibited a significantly poorer fit, $\chi^2/N \approx 6.5$. The fitting parameters obtained from these analyses, together with the respective volume integrals and χ^2/N values, are listed in Table III.

In Fig. 6 the volume integral, $J_R/4A$, obtained in this work is compared with the values given in Refs. 10 and 27. The results suggest that J_R exhibits either a constant or weakly nonlinear energy dependence over the laboratory energy range from 47 to 200 MeV. On the basis of our result at 198.4 MeV, the linear energy dependence postulated in Ref. 10 does not appear to be imperative.

If the phenomenological potentials are considered as local, l-dependent equivalents to the completely antisymmetrized solution based on the resonating group method (RGM, or its simplified version, the orthogonality condition model), then the weak energy dependence of the real volume integral can be attributed to the dominant role played by the Pauli exclusion principle and exchange effects in the elastic $\alpha+\alpha$ channel. For low partial waves such equivalent potentials should produce radial wave functions with correct RGM nodal behavior, e.g., the $l=0$ continuum wave function should have at least two nodes in the overlap region which correspond to the two forbidden $\alpha+\alpha$ S-wave states. At $E_{\rm lab}=198.4$ MeV the $l=0$ radial wave function for the WS1 + WS2 potential exhibits nodes at $r_n=0.75$, 1.5, and 2.3 fm. The locations of the first two nodes are nearly identical to the values determined by Neudatchin[25] at $E_{\rm lab}=86$ MeV; $r_n=0.7$, 1.6, and 2.75 fm, and are only slightly smaller than those calculated by Okai and Park[28] at $E_{\rm lab}=30$ MeV, $r_n\cong 0.8$ and 1.9 fm. This consistency suggests that the nodal behavior of the relative $l=0$ $\alpha+\alpha$ wave function is almost energy independent, as expected if Pauli exclusion effects dominate the N-N dynamics of the α-α interaction.[26]

V. SUMMARY

In summary, these measurements have demonstrated that the $\alpha+\alpha$ reaction does not lead to overproduction of ^{6}Li in galactic-cosmic-ray interactions with the interstellar medium. Hence, the GCR + ISM model appears to be able to account for nature's ^{6}Li, ^{9}Be, ^{10}B, and ^{11}B satisfactorily. In contrast, ^{7}Li is underproduced by an order of magnitude; this amount can be self-consistently provided by cosmological nucleosynthesis in the big bang, provided one assumes the maximum uncertainties in the primordial ^{7}Li abundance of Spite and Spite.[21] The amount of cosmological ^{7}Li required to yield the natural ^{7}Li/^{6}Li ratio is consistent with an expanding (open) universe, assuming the neutrino mass is small.

In addition, $\alpha+\alpha$ elastic scattering data obtained in this experiment have been analyzed in terms of an optical model which employs two different parametrizations: a standard Woods-Saxon potential and the sum of two Woods-Saxon potentials. The latter approach yields the superior fit. The real volume integral obtained in this analysis indicates a nearly energy-independent behavior over the laboratory energy range from 47 to 200 MeV. This can be taken as evidence of the influence of the Pauli exclusion principle on the reaction dynamics in $\alpha+\alpha$ collisions.

ACKNOWLEDGMENTS

The authors wish to thank Sam M. Austin for his contributions toward initiating these experiments and subsequent discussions of the results. We are indebted to T. P. Walker for providing us with the results of his GCR nucleosynthesis calculations prior to publication. T. E. Ward and M. L. Walker are acknowledged for their involvement in the early stages of this work, as is Terry Sloan for his assistance with the 64-inch scattering chamber. Dennis Friesel and the IUCF operating crew provided excellent beams during these experiments. This work was supported by the National Science Foundation and the U.S. Department of Energy.

*Present address: Institute of Atomic Energy, Academia Sinica, Beijing, People's Republic of China.

[1]Sam M. Austin, Prog. Part. Nucl. Phys. **7**, 1 (1981).
[2]R. V. Wagoner, Astrophys. J. **179**, 343 (1973); R. V. Wagoner, W. A. Fowler, and F. Hoyle, *ibid.* **148**, 3 (1967).
[3]H. Reeves, W. A. Fowler, and F. Hoyle, Nature **226**, 727 (1970).
[4]S. M. Read and V. E. Viola, At. Data Nucl. Data Tables **31**, 359 (1984).
[5]C. H. King, H. H. Rossner, Sam. M. Austin, W. S. Chien, G. H. Mathews, V. E. Viola, Jr., and R. G. Clark, Phys. Rev. Lett. **35**, 988 (1975).
[6]C. H. King, Sam M. Austin, H. H. Rossner, and W. H. Chien, Phys. Rev. C **16**, 1712 (1977).

[7]B. G. Glagola, V. E. Viola, Jr., H. Breuer, N. S. Chant, A. Nadasen, P. G. Roos, Sam M. Austin, and G. J. Mathews, Phys. Rev. C **25**, 34 (1982).

[8]F. Yiou and G. M. Raisbeck, in *Proceedings of 15*th *International Cosmic Ray Conference,* Plovdiv, 1977, edited by B. Betov (Bulgarian Academy of Sciences, Sofia, 1977), p. 133.

[9]C. T. Roche, R. G. Clark, G. J. Mathews, and V. E. Viola, Phys. Rev. C **14**, 410 (1976); R. A. Moyle, B. G. Glagola, G. J. Mathews, and V. E. Viola, Jr., *ibid.* **19**, 631 (1979).

[10](a) A. Nadasen, P. G. Roos, B. G. Glagola, G. J. Mathews, V. E. Viola, Jr., H. G. Pugh, and P. Frisbee, Phys. Rev. C **18**, 2792 (1978); (b) A. Gökmen, H. Breuer, A. C. Mignerey, B. G. Glagola, K. Kwiatkowski, and V. E. Viola, Jr., Phys. Rev. C **29**, 1595 (1984).

[11]N. S. Chant, Nucl. Phys. **A211**, 269 (1973).

[12]D. Bodansky, W. W. Jacobs, and D. L. Oberg. Astrophysical J. **202**, 222 (1975).

[13]T. P. Walker, G. J. Mathews, and V. E. Viola, Jr., submitted to Astrophysical J.

[14]M. Meneguzzi, J. Audouze, and H. Reeves, Astron. Astrophys. **15**, 337 (1971).

[15]H. E. Mitler, Astrophys. Space Sci. **17**, 186 (1972).

[16]A. G. W. Cameron, in *Essays in Nuclear Astrophysics,* edited by C. Barnes, D. Clayton, and D. Schramm (Cambridge University Press, Cambridge, 1982), p. 35.

[17]E. Anders and M. Ebihara, Geochim. Cosmochim. Acta **46**, 2363 (1982).

[18]A. M. Boesgaard, Publ. Astron. Soc. Pac. **88**, 353 (1976).

[19]J. P. Meyer, in *Proceedings of the 22*nd *Liege International Astrophysics Symposium,* 1978.

[20]H. Reeves and J. P. Meyer, Astrophys. J. **226**, 613 (1978).

[21]F. Spite and M. Spite, Astron. Astrophys. **115**, 357 (1982); M. Spite and F. Spite, Nature **297**, 483 (1982).

[22]G. Beaudet and A. Yahill, Astrophys. J. **218**, 253 (1977).

[23]J. Yang, M. S. Turner, G. Steigman, D. N. Schramm, and K. A. Olive, Astrophys. J. **281**, 493 (1984).

[24]G. J. Mathews and V. E. Viola, Astrophys. J. **228**, 375 (1979).

[25]V. G. Neudatchin, V. I. Kukulin, V. L. Korotkich, and V. P. Korennoy, Phys. Lett. **34B**, 58 (1971); V. I. Kukulin, V. G. Neudatchin, and Yu. F. Smirnov, Nucl. Phys. **A245**, 429 (1975).

[26]B. Buck, H. Friedrich, and C. Wheatly, Nucl. Phys. **A275**, 246 (1977).

[27]G. T. C. van Niftrik *et al.,* C. R. Congr. Int. Phys. Nucl. **1964**, 858 (1964).

[28]S. Oaki and S. C. Park, Phys. Rev. **145**, 787 (1966).